

Fig. 3 showed no iron loss.

17. R. N. Schock, A. G. Duba, T. J. Shankland, *J. Geophys. Res.* **94**, 5829 (1989); S. Constable and J. J. Roberts, *Phys. Chem. Miner.* **24**, 319 (1997).
18. H. St. C. O'Neill et al., *Am. Mineral.* **78**, 456 (1993).
19. B. Kamb, *ibid.* **53**, 1439 (1968).
20. G. Nover, G. Will, R. Waitz, *Phys. Chem. Miner.* **19**, 133 (1992).
21. H. Horiuchi, M. Akaoki, H. Sawamoto, in *High-Pressure Research in Geophysics*, S. Akimoto and M. H. Manghnani, Eds. (Center for Academic Publications, Tokyo, 1982), pp. 391–403.
22. A. E. Ringwood, *Composition and Petrology of the Earth's Mantle* (McGraw-Hill, New York, 1975), p. 618; T. Irifune and A. E. Ringwood, *Earth Planet. Sci. Lett.* **86**, 365 (1987).
23. E. Ito and T. Katsura, *Geophys. Res. Lett.* **16**, 425 (1989).
24. D. L. Turcotte and G. Schubert, *Geodynamics: Applications of Continuum Physics to Geological Problems* (Wiley, New York, 1982).
25. T. J. Shankland, J. Peyronneau, J.-P. Poirier, *Nature* **366**, 453 (1993) [SPP93].
26. We thank A. G. Duba and H. Xie for discussions and

suggestions; H. Fischer, K. Klasinski, H. Kufner, and R. Weigel for technical assistance; and H. Schulze for making the thin sections. D. L. Kohlstedt (University of Minnesota) donated sample materials. Electron microprobe analyses were performed with the assistance of D. Kraube, and C. McCammon and S. Lauterbach did the Mössbauer analyses of the samples. T.J.S. thanks the Alexander von Humboldt Foundation and the Office of Basic Energy Sciences of the U.S. Department of Energy for support.

28 January 1998; accepted 23 March 1998

In Situ Discovery of Graphite with Interstellar Isotopic Signatures in a Chondrule-Free Clast in an L3 Chondrite

S. Mostefaoui, P. Hoppe, A. El Goresy*

Optical and scanning electron microscopy of a chondrule-free clast in the unequilibrated L3 chondrite Khohar revealed a spherical object consisting of an aggregate of small (~2-micrometer diameter), Ni-poor (0.5 to 2.89 weight percent) metal particles and fine-grained graphite (<1-micrometer diameter). The graphite has large D and ¹⁵N excesses (δD ~ 1500 per mil and δ¹⁵N ~ 1300 per mil) with two isotopically distinct signatures: N rich with a high D/H ratio and N poor with a high ¹⁵N/¹⁴N ratio. These excesses are the largest D and ¹⁵N excesses observed in situ in a well-characterized phase in a meteorite. The isotopic characteristics are suggestive of an interstellar origin, probably by ion-molecule reactions at low temperature in the interstellar molecular cloud from which the solar system formed. The structure and nonchondritic composition of the metal particles suggest they did not form under equilibrium conditions in the solar nebula.

Different graphite morphologies (1) have been observed in many unequilibrated chondrites (2, 3). In the unequilibrated ordinary chondrite Khohar (UOC L3 type) and the Acfer-182 carbonaceous chondrite of Renazzo type (CR), large ¹⁵N and D excesses were measured in mixtures of fine-grained graphite and graphite books (book refers to a structure of parallel sheets) (2). The large size of the books permitted analysis of individual grains by secondary ion mass spectrometry (SIMS). The H and N isotopic compositions did not indicate any ¹⁵N or D excesses; however, we could not analyze the different fine-grained graphite grains separately because the graphite grain types are mixed with the graphite books. To determine if the fine-grained graphite grains are the source of the ¹⁵N and D anomalies, we searched for assemblages that contained only the fine-grained graphite to analyze for C, N, and H isotopic compositions.

In a fine-grained chondrule-free clast in the Khohar chondrite (Fig. 1A) we found a

S. Mostefaoui and A. El Goresy, Max-Planck-Institut für Kernphysik, Postfach 103980, 69029 Heidelberg, Germany.

P. Hoppe, Physikalisches Institut, Universität Bern, Sidlerstrasse 5, CH-3012 Bern, Switzerland, and Max Planck-Institut für Chemie, Postfach 3060, D-55020 Mainz, Germany.

*To whom correspondence should be addressed. E-mail: goresy@pluto.mpi-hd.mpg.de

spherical object (~100 μm in diameter) consisting of an unaltered fine-grained, Ni-poor metal aggregate and graphite (Fig. 1B). This spherule does not have layers surrounding it, and the graphite was found to be all fine grained. We analyzed the whole clast for its bulk chemical composition with the electron microprobe (EMP) broad-beam technique. The graphite-bearing metal spherule was then surveyed with a scanning electron microscope (SEM), and the metal phases were analyzed for Fe, Ni, Co,

Cr, Si, P, and S by wavelength-dispersive EMP techniques. The isotopic compositions of H, C, and N of the graphite were measured by SIMS.

The clast is about 2 mm in diameter and essentially chondrule free (Fig. 1A). Because the clast is located at the edge of the meteorite section, its original size was probably larger. The clast consists mostly of small (<10 μm) silicate grains and metal particles, with some large metal grains (~100 μm) and two glass grains (~300 μm) (Fig. 1A). The bulk chemical composition of the clast (Table 1), obtained by 20 broad-beam EMP analyses, is different from the bulk compositions of both the Khohar chondrite and the L ordinary chondrite group (4). The abundances of the major oxides SiO₂, MgO, and FeO are similar to those of the bulk composition of the Orgueil (CI) carbonaceous chondrite (Table 1).

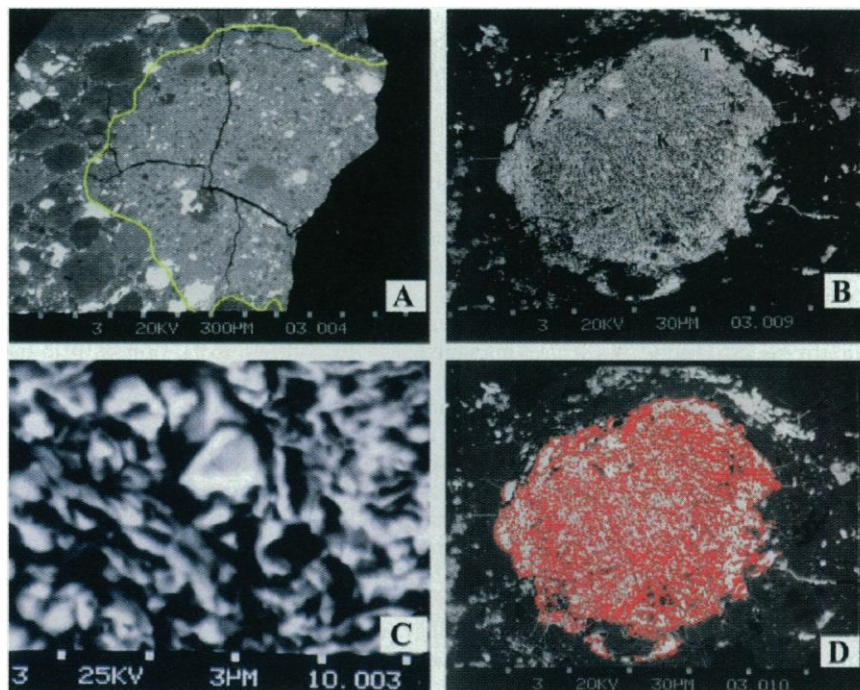
The metal-graphite assemblage in the clast (Fig. 1, B and C) consists of small (≤2 μm) metal particles of kamacite and taenite and fine-grained (<1 μm) birefringent graphite (5). Detailed examination of the metals with high-resolution BSE imaging with the SEM revealed no sign of alteration of the metal. The graphite is abundant and fills interstices between the metal particles (Fig. 1D). We estimated the total amount of C in the assemblage to be about 50 volume %. This much graphite with its

Table 1. The bulk chemical composition of the chondrule-free clast in the Khohar (L3) chondrite. The Khohar chondrite, L group ordinary chondrites (OCs), and Orgueil (CI) carbonaceous chondrite bulk chemical compositions are shown for comparison.

Compound	Khohar clast		Orgueil (bulk)	Khohar (bulk)	L group OCs (bulk)
	Range	Average			
SiO ₂	37.24–44.41	40.82	37.90	46.71	46.7
TiO ₂	0.11–1.37	0.21	0.12	0.13	0.14
Al ₂ O ₃	2.39–3.49	2.87	2.84	2.70	2.64
Cr ₂ O ₃	0.48–0.85	0.69	0.53	0.61	0.62
FeO	22.54–26.66	25.07	28.11	16.83	17
MnO	0.36–0.47	0.42	0.35	0.41	0.4
MgO	24.61–27.22	26.11	26.51	29.31	29.07
CaO	0.56–3.59	1.38	2.27	2.11	2.17
Na ₂ O	0.53–1.03	0.77	1.27	1.05	1.12
K ₂ O	0.20–0.46	0.36	0.10	0.12	0.13
Total	97.54–101.52	98.71	100.00*	100.00*	100.00*

*Recalculated from (4), after subtraction of H₂O, P₂O₅, C, FeS, and Fe-Ni-Co metal.

Fig. 1. (A) SEM backscattered electron (BSE) image of a region of the Khohar (L3) chondrite containing a chondrule-free clast. The clast (delimited by the yellow line) is composed of small silicate and metal grains ($<10\ \mu\text{m}$). Rare, large metal grains (white patches, $\sim 100\ \mu\text{m}$) are visible, as are two glass patches (dark gray patches, $\sim 300\ \mu\text{m}$) in the center. (B) BSE image of a spherical object in the clast consisting of $<2\text{-}\mu\text{m}$ Fe-Ni metal particles and fine-grained ($<1\ \mu\text{m}$) graphite with interstellar isotopic signatures. The metal occurs in two phases: kamacite (K), which is abundant and found mostly in the center of the object, and taenite (T), which is rare and present in the outer part. (C) Enlarged area of the assemblage in (B). The kamacite particles have different levels of brightness, indicating differences in Ni contents. Some of the particles in this area are nearly pure metallic iron (Fe $\sim 99.5\%$). (D) The graphite in (B) was digitally colored red. The graphite is abundant (>50 volume % total C in the assemblage) and fills interstices between the metal particles, thus appearing as a branching network of tiny flakes. The scale numbers [300 μm in (A), 30 μm in (B) and (D), and 3 μm in (C)] correspond to the distances between the marks.



coexisting metal particles is unlikely to be produced by the breakdown of carbides. The only detectable elements in the metal are Fe, Ni, and Co. The Co content in the taenite is ~ 0.89 weight %, whereas in the kamacite it is below the detection limit (<0.01 weight %). This represents a large difference in the chemical composition of the Fe-Ni metals compared with other ordinary chondrites (6). In addition, kamacite and taenite are Ni poor (0.5 to 2.89 weight % and 28 to 32 weight %, respectively) compared with kamacite and taenite Ni compositions in other ordinary chondrites (6). BSE images of the metal with the SEM showed that the kamacite particles display different levels of brightness, indicating variations in Ni concentrations. Although, these particles are too small to be individually analyzed with an EMP, quantitative analysis in different areas (comprising bright and dark particles) showed variations in Ni concentrations of up to a factor of 3. The electron beam of the SEM is smaller than the size of the kamacite particles, and analysis of the individual particles revealed that the darker particles have Ni contents as low as ~ 0.5 weight %. X-ray energy spectra of these particles showed no carbon K_{α} line, which indicates that these particles are not carbides, but rather, nearly pure metallic Fe.

We analyzed the graphite in the assemblage by SIMS for its C, N, and H isotopic compositions and H and N concentrations. The measurements were done with a Cs^+ primary ion beam of 3 to 5 μm in diameter. Because graphite particles are $<1\ \mu\text{m}$ in

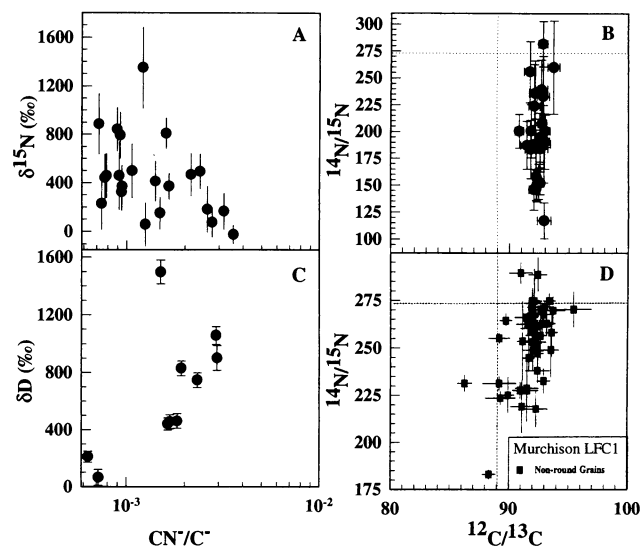
size, the measurements only provide an average composition of the graphite mixtures. Because the analysis of H and the analysis of C and N require different settings of the ion microprobe, the C and N isotopes were measured simultaneously and independently from the H isotopes.

The maximum H and N concentrations in the graphite are 4100 and 250 ppm, respectively, although most analyses gave lower concentrations. These concentrations were estimated from the measured H^-/C^- and CN^-/C^- ion ratios as described in (7). The C isotopic ratios are not significantly different from the terrestrial Pee Dee be-

lemnite (PDB) standard ratio (Fig. 2B), and $\delta^{13}\text{C}$ values lie between -21 per mil and -51 per mil, indicating isotopically light graphite. The N isotopic ratios, on the other hand, are more variable and anomalous, with $\delta^{15}\text{N}$ values of up to 1330 per mil (Fig. 2A). There is no correlation between the N and C isotopic ratios (Fig. 2B). The highest $\delta^{15}\text{N}$ values were found in graphites with low N concentrations [expressed as CN^-/C^- ion ratios (Fig. 2A)].

The H isotopic ratios are also variable (Fig. 2C), with positive δD (8) values that range from close to normal ($\delta\text{D} = 0$ per mil) up to anomalous ($\delta\text{D} = 1500$ per mil).

Fig. 2. (A to C) The C, N, and H isotopic compositions of graphite in the metal assemblage in the Khohar clast. (A) $\delta^{15}\text{N}$ [in per mil (‰)] as a function of N concentrations expressed as CN^-/C^- ion ratios. (B) C versus N isotopic ratios. All $^{12}\text{C}/^{13}\text{C}$ ratios are higher than the terrestrial PDB standard ratio (the horizontal and vertical dashed lines are respectively the terrestrial $^{12}\text{C}/^{13}\text{C}$ and $^{15}\text{N}/^{14}\text{N}$ ratios), thus indicating isotopically lighter graphite. (C) Hydrogen isotopic composition as a function of CN^-/C^- ion ratios. (D) The isotopic signatures of $<1\text{-}\mu\text{m}$ graphitic grains analyzed by Zinner *et al.* (9) from Murchison.



In addition, there is a tendency for δD to increase with increasing N content. The highest δD values are found in graphites with high N concentrations ($CN^-/C^- > 1.6 \times 10^{-3}$) (Fig. 2C). This indicates the presence of either two distinct types of graphite, one N rich with high D abundance and the other N poor with high ^{15}N content, or one graphite type mixed with isotopically different nongraphitic carbonaceous material.

The D and ^{15}N excesses reported here are the largest D and ^{15}N excesses measured in situ in a well-characterized phase in a meteorite. The isotopic characteristics are of an interstellar origin. The lack of C isotopic anomalies along with ^{15}N excesses (Fig. 2B) are similar to the isotopic signatures of the $<1\text{-}\mu\text{m}$ nonround graphitic grains found in graphite residues of the Murchison carbonaceous chondrite (9) (Fig. 2D). They also resemble those of many interplanetary dust particles (10). The ^{15}N and D excesses in the graphite from Murchison and the interplanetary dust particles might be derived from an interstellar molecular cloud (IMC) (9, 10). The narrow range in $^{12}C/^{13}C$ ratios in graphite in the Khohar assemblage, in comparison with the C isotopic ratios of the graphite from Murchison (Fig. 2, B and D), suggests that the Khohar clast probably sampled a specific region from an IMC.

Fractionation processes occurring in IMCs can lead to D and ^{15}N enrichments in H- and N-bearing molecules (11, 12). Ion-molecule reactions in IMCs involve a large number of molecular species (13, 14). This, and the low-temperature reaction kinetics, makes the chemistry of the IMC complex (15). In the early 1980s, considerable interest was devoted to the H chemistry in IMC environments. Elevated D/H ratios have been directly observed in many species, in-

cluding HCN, NH_3 , CH_4 , H_2O , H_3^+ , CH_3^+ , and HCO^+ (16). In HCN molecules, D/H ratios can be more than 100 times as high as those in the solar system [(16) and references therein] and more than 40 times as high as the ratios measured in the Khohar graphite. We always analyzed a large number of graphite grains simultaneously, which may reduce the maximum D/H ratios of single grains; however, the isotopic effects of single graphite grains may be larger than measured.

In contrast to H, only a little has been done on N chemistry. To explain the enrichments in ^{15}N observed in IMCs, Adams and Smith (12) measured enhancements of $^{15}N/^{14}N$ in N_2H^+ , relative to N_2 , of 2.5 and 1.6 at 10 K and 20 K, respectively. In NH_3 molecules detected in the direction of Orion-KL, Hermsen *et al.* (17) estimated the enhancement of ^{15}N to about a factor of ~ 1.6 relative to the solar system $^{15}N/^{14}N$ ratio.

Graphite is considered an important constituent of carbonaceous dust detected in the interstellar medium (18). The anisotropism observed with the optical microscope in the Khohar assemblage indicates that most of the C is present as crystalline graphite. However, although all or most of the C in the assemblage is graphite, we do not know in which forms H and N are sited in the graphite; therefore, the enrichments in D and ^{15}N may not be genetically associated with the graphite. Some portions of the Khohar chondrite show different signs of shock (19), and it has been postulated that shock waves can induce the redistribution of volatile elements by evaporation and recondensation (20). The scenario proposed in (20) would also call for the release of elements like H and N by shock waves from their original D- and ^{15}N -rich phases. It is then expected that they will get trapped in graphite of solar system origin. Woolum and Burnett (20) reported enrichments in Bi and Pb in a Ni-poor metal fraction (~ 2 weight % Ni) in Khohar and explained this as a consequence of shock waves. However, such a scenario predicts a positive correlation between ^{15}N and D enrichments because, if they get trapped in graphite after they were released from their original phases as a result of the shock waves, N and H should be randomly or quasi-homogeneously redistributed. The H and N isotopic signatures in the Khohar assemblage are not correlated. In addition, the metal assemblage as well as the other metal grains in the clast do not show any shock metamorphic effects, either in the texture or in the chemical composition. Therefore, we argue that, although the chondritic part in Khohar shows different degrees of shock metamorphism, the N and

H isotopic compositions in the graphite in the clast were not generated by a dynamic impact event.

The presence of metal particle having nonchondritic chemical composition with particles of nearly pure metallic iron (Fig. 1C), as well as their association with graphite having interstellar isotopic signatures was unexpected. To determine if the kamacite and taenite formed under conditions of equilibrium, we compared the compositions of the Khohar metals with experimental data for the Fe-Ni-Co system at equilibrium (21). The compositions of the metal in the graphite-metal spherule plot far away from the trend obtained from experimental equilibration (Fig. 3). This suggests that the metal particles are out of equilibrium. The assemblage in the Khohar clast is probably an agglomerate of metal particles and graphite from different sources that mixed and compacted to form this spherical object. The mechanism, location, and period of mixing are unknown. Such clasts with no chondritic features are good candidates for an in situ search for extrasolar material.

REFERENCES AND NOTES

1. The graphite morphologies include spherulitic, books, cliftonite (polycrystalline aggregate with cubic morphology), and a very fine-grained ($<1\ \mu\text{m}$) type.
2. S. Mostefaoui, E. Zinner, P. Hoppe, A. El Goresy, *Lunar Planet. Sci.* **XXVIII**, 989 (1997).
3. S. Mostefaoui, thesis, Muséum National d'Histoire Naturelle Paris (1996).
4. E. Jarosewich, *Meteoritics* **25**, 323 (1990).
5. The birefringence of the graphite can be seen by using crossed nichols in a polarizing reflected light optical microscope.
6. F. Afittalab and J. T. Wasson, *Geochim. Cosmochim. Acta* **44**, 431 (1980).
7. P. Hoppe *et al.*, *ibid.* **59**, 4029 (1995).
8. $\delta D = [(D/H)_{\text{sample}}/(D/H)_{\text{SMOW}}] \times 100$, where SMOW is the terrestrial standard, standard mean ocean water, and units are parts per thousand.
9. E. Zinner *et al.*, *Meteoritics* **30**, 209 (1995).
10. S. Messenger and R. M. Walker, in *Astrophysical Implications of the Laboratory Study of Presolar Materials* (American Institute of Physics, Woodbury, NY, 1997), pp. 545–564.
11. J. Geiss and P. Bochsler, *Geochim. Cosmochim. Acta* **46**, 529 (1982).
12. N. G. Adams *et al.*, *Astroph. J.* **247**, L123 (1981).
13. S. S. Prasad and W. T. Huntress Jr., *Astrophys. J. Suppl.* **43**, 1 (1980).
14. ———, *Astrophys. J.* **239**, 151 (1980).
15. W. D. Langer and T. E. Graedel, *Astrophys. J. Suppl.* **69**, 241 (1989).
16. T. J. Millar, A. Bennett, E. Herbert, *Astrophys. J.* **340**, 906 (1989).
17. W. Hermsen, T. L. Wilson, C. M. Walmsley, W. Batrla, *Astron. Astrophys.* **146**, 134 (1985).
18. A. G. G. M. Tielens, in *Carbon in the Galaxy: Studies from Earth and Space*, J. C. Tarter, S. Chang, D. J. Defrees, Eds. (NASA Conf. Publ. 3061, Washington, DC, 1990), pp. 59–111.
19. A. Bischoff and D. Stöffler, *Eur. J. Mineral.* **4**, 707 (1992).
20. D. S. Woolum and D. S. Burnett, *Geochim. Cosmochim. Acta* **45**, 1619 (1981).
21. S. Widge *et al.*, *Trans. Met.* **8A**, 309 (1977).
22. We are grateful to J. Janicke, V. Träumer, C. Klehr, and G. Bonk for technical assistance.

12 January 1998; accepted 13 April 1998

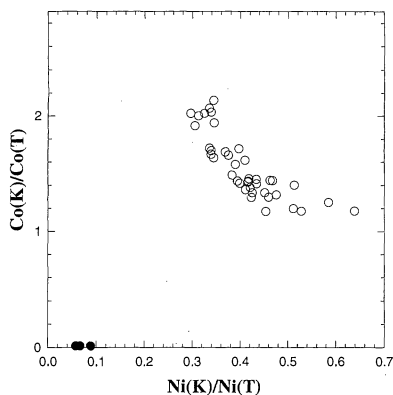


Fig. 3. Ni as a function of Co concentration ratios in the two coexisting metallic phases kamacite (K) and taenite (T) in the assemblage (filled circles) compared with the experimental results for the Fe-Ni-Co system at equilibrium (open circles) (21).